Magnetic structure of $Gd_5Si_2Ge_2$ and $Gd_5Si_2Ge_{1.9}M_{0.1}$ (M = Ga, Cu)

2010 J. Phys.: Condens. Matter 22 446003

(http://iopscience.iop.org/0953-8984/22/44/446003)

J. Phys.: Condens. Matter **22** (2010) 446003 (6pp) doi:10.1088/0953-8984/22/44/446003

Magnetic structure of $Gd_5Si_2Ge_2$ and $Gd_5Si_2Ge_{1.9}M_{0.1}$ (M = Ga, Cu)

E Palacios[1], J A Rodríguez-Velamazán[1,2], G F Wang[1], R Burriel[1], G Cuello[2] and J Rodríguez-Carvajal[2]

[1] Instituto de Ciencia de Materiales de Aragón, Departamento de Física de la Materia Condensada, CSIC-University of Zaragoza, Pedro Cerbuna 12, 50009 Zaragoza, Spain
[2] Institute Laue-Langevin, 6 rue Jules Horowitz, 38000 Grenoble, France

E-mail: elias@unizar.es

Received 16 July 2010, in final form 6 September 2010
Published 22 October 2010
Online at stacks.iop.org/JPhysCM/22/446003

Abstract

Powder x-ray diffraction patterns of the doped compounds $Gd_5Si_2Ge_{1.9}M_{0.1}$ (M = Ga, Cu) show the same crystal structure, orthorhombic Gd_5Si_4-type, in the ferromagnetic and paramagnetic phases. This is different from $Gd_5Si_2Ge_2$, whose paramagnetic phase is monoclinic. The magnetic structure at low temperature, solved from diffraction experiments with hot neutrons, is the same in all the three compounds, collinear ferromagnetic with moments along the crystal *b*-axis, or F_yF_{By} according to Bertaut's notation. These results, combined with those of heat capacity and magnetocaloric effect, indicate, similarly to Gd_5Si_4, a second-order, purely magnetic, transition in the doped compounds explaining the absence of hysteresis.

(Some figures in this article are in colour only in the electronic version)

1. Introduction

Since the discovery of the 'giant magnetocaloric effect' (GMCE) in 1997 by Pecharsky and Gschneidner [1], many families of compounds have been studied, with respect to their potential technical applications in magnetic refrigeration near room temperature. For studies until 2003 we refer the reader to the monograph by Tishin and Spichkin [2]. A review on the Mn based GMCE compounds has been published by Brück *et al* [3]. The first family discovered, $Gd_5(Si_xGe_{1-x})_4$ ($0.2 < x < 0.5$), is by far the most studied one and remains among the most efficient GMCE materials. More than one hundred papers about it have been published in the last decade. In these compounds, the GMCE is due to the simultaneous magnetic and structural first-order transition from an orthorhombic ferromagnetic phase O(I) (Gd_5Si_4-type) to a monoclinic paramagnetic phase, M. Figure 1 shows a temperature/composition phase diagram at zero field. The transition temperature T_C can be tuned between 140 and 270 K by selecting the Si/Ge ratio. At higher temperatures and zero field the O(I) structure is recovered, now in paramagnetic state [4]. Si-rich compositions (i.e. $x > 0.5$) have only a magnetic transition with T_C increasing slowly from 295 K for $x \to 0.5$ to 335 K for $x = 1$. On the opposite end of the composition–temperature phase diagram, for $x < 0.2$ the ferromagnetic O(I) phase transforms first into an antiferromagnetic Sm_5Ge_4-type structure, O(II), and this undergoes a magnetic transition to paramagnetic near 125 K. The O(I) and O(II) phases have the same space group, *Pnma*, and similar cell constants, but quite different atomic positions, so they are usually considered as different structure types. The main qualitative difference between the O(I) and O(II) phases is the distance between Si or Ge atoms on 8d sites, which changes from ca 3.5 Å in O(II) to ca 2.6 Å in O(I) [7], allowing the formation of dimers in this last phase. In the M phase, one half of the dimers are broken. These structural changes modify the exchange interactions and therefore determine the different magnetic structures and ordering temperatures.

In spite of the many works published on $Gd_5(Si, Ge)_4$, the magnetic structure has not been directly determined. Usually, considerations about it have been extrapolated from results in other rare earth compounds, like $Tb_5(Si, Ge)_4$ [8], or $Er_5(Si, Ge)_4$ [9]. However, the Gd atom has zero orbital angular momentum and the magnetic properties are not affected by the crystal field in the same way as in other rare earth atoms. The difficulty for a magnetic structure determination via neutron diffraction lies in the huge cross section, σ_a, of the natural Gd for the absorption of thermal neutrons. For a typical powder neutron diffraction experiment with wavelength $\lambda = 1.8$ Å, $\sigma_a = 48.8 \times 10^3$ barn [10], which

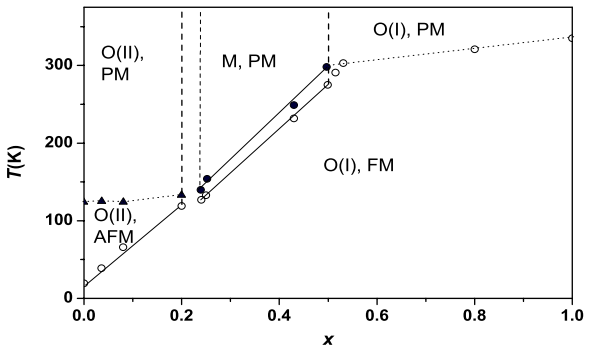

Figure 1. Temperature/composition phase diagram at zero field for $Gd_5(Si_xGe_{1-x})_4$, from [5] and [6]. Open circles: transition to the ferromagnetic (FM) O(I) phase on cooling. Solid circles: transition to the paramagnetic (PM) M phase on heating. Triangles: transition between antiferromagnetic (AFM) and paramagnetic phases. Solid lines: first-order transitions. Dotted lines: second-order transitions. Dashed lines: borders of different crystal structures in the paramagnetic state. Between the M and O(II) phases there is a narrow two-phase region.

gives a penetration depth $L = 8.2$ μm in solid $Gd_5(Si, Ge)_4$. Using hot neutrons the absorption can be reduced to still high but tolerable values. Using by instance, $\lambda = 0.5$ Å, gives $\sigma_a = 760$ barn [11] and $L = 0.53$ mm. On the contrary, the resolution is not always enough to get single Bragg peaks in a powder neutron diffraction experiment with this short wavelength. Nevertheless, even complex magnetic structures in, e.g., $GdNi_2Si_2$, $GdCu_2Si_2$ [12] and GdCu [13] have been solved using hot neutron powder diffraction.

Regarding applications in magnetic refrigeration, the main drawback of $Gd_5Si_2Ge_2$ is the large hysteresis, which imposes a minimum initial applied field near 2 T to achieve a complete isothermal ferromagnetic to paramagnetic transition, even at the most favourable temperature. Recently it has been reported that replacing (doping) a small amount of Ge by some other metal (Fe, Co, Cu, Ga, Mn, Al) reduces or even eliminates the hysteresis, keeping or increasing the net refrigeration capacity [14, 15]. We have chosen to study the effect of doping with non-magnetic Ga and Cu. The aim of this work is to study the crystal structures and the low temperature magnetic structures of the title compounds.

2. X-ray diffraction

The samples used in this study were the same as used previously for SEM, magnetic [15] and thermal measurements [16]. These results suggest a second-order transition at $T_C = 293.6$ K for the Ga-doped compound. For the Cu-doped compound our heat capacity experiments show a very similar behaviour with $T_C = 294$ K. In addition to previous experimental work, the samples were analysed by x-ray fluorescence and diffraction (XRD) between 200 and 350 K. XRD patterns were collected in a rotating anode RU 300, operated at 80 mA. The data collection was performed every 0.03° using a goniometer Rigaku/Max System. Figure 2 (left) shows the XRD pattern of $Gd_5Si_2Ge_{1.9}Ga_{0.1}$ at 250 and 350 K. In addition to the main phase there is 3.7% in mass of $Gd(Si, Ge)_1$ (1:1 alloy) and 14.4% of $Gd_5(Si, Ge)_3$ (5:3 alloy). The same phases were found in the Cu-doped and in the non-doped compounds, with similar proportions. These proportions are consistent with the global analysis performed by x-ray fluorescence and with previous analysis. The structural data were taken from the literature for the nearest compositions [4, 18–20]. The $Gd_5Si_2Ge_2$ patterns were compatible with the M phase at room temperature and at 350 K. At 250 K the structure is O(I) type. For the doped compounds, a previous analysis of the structure at RT (i.e. some undetermined temperature between 290 and 300 K) was not conclusive to assess whether the paramagnetic phase is M or O(I) type, because of the proximity of the magnetic transition. Rietveld analysis was carried out for patterns at several temperatures, in ferromagnetic and paramagnetic phases (figure 2). The doped compounds have the O(I) structure for temperatures below 350 K. This is similar to the Si-rich alloys in $Gd_5(Si_xGe_{1-x})_4$ with $x > 0.5$. In the Cu-doped compound, the only difference between the 350 K pattern and the 200 K one is the appearance of two small peaks at $2\theta = 31.2°$ and 32.6°. They correspond to the $(2\bar{3}1)$, $(1\bar{3}2)$ (very closely spaced) and (231) reflections, among the most intense for the M phase. That would indicate some inhomogeneity in composition, the proportion of Cu being too low to avoid the first-order O(I)–M transition and/or the Ge proportion being higher than the nominal value in some small parts of the sample.

3. Neutron diffraction

The neutron diffraction (ND) experiment was carried out on the D4 diffractometer [17] at the Institut Laue-Langevin, Grenoble (France). This instrument uses a hot neutron source and a Cu-(220) monochromator providing neutrons of wavelength $\lambda = 0.4964$ Å. The scattered intensity is collected by a bank of nine multi-detectors of 64 ^{3}He cells in steps of 0.125°, covering 8° each, with gaps of 7° between two adjacent multi-detectors. Every full pattern was collected by positioning the bank (position of the first cell of the first multi-detector) at 0°, 4°, 8° and 12°. The background radiation coming from parts of the cryostat lying out of the focusing centre is shadowed by the collimators for some detector cells, depending on the position of the bank, which produces some jumps in the experimental diffraction pattern. To correct for this effect, taking into account the absorption by the sample, a pattern was collected on an empty sample holder and another one with a sample of pure boron, considered as completely absorbent. The corrected intensity at a given angle 2θ is approximated by $y_{corr} = y_{exp} - \eta y_h + (1 - \eta) y_B$, where y_{exp} is the experimental intensity, properly weighted over the positions of the bank and efficiency of every cell. y_h and y_B are the intensities for the empty holder and for boron, respectively. η is a fitting parameter between 0 and 1. The geometry of the sample is not exactly the same as that of boron, therefore some jumps appear in the patterns (for instance at $2\theta = 4.625°$) even with the best choice of η. These jumps are not related to any property of the sample but, as mentioned, to the different shadowing of the ambient neutron radiation by the collimators, for different detectors.

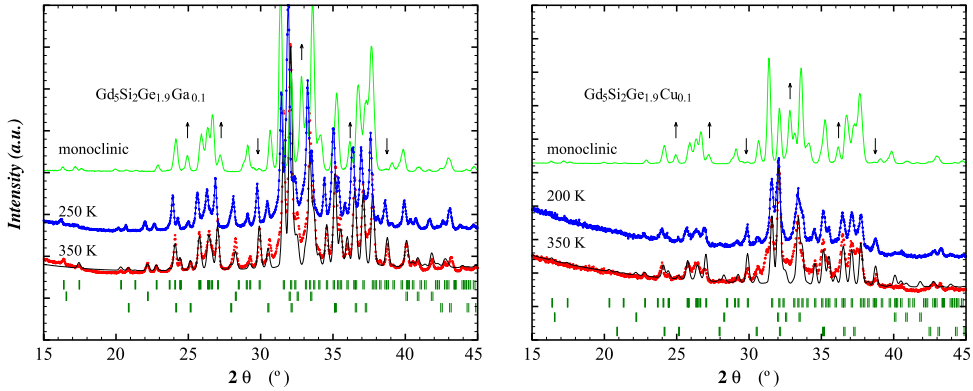

Figure 2. X-ray diffraction patterns of $Gd_5Si_2Ge_{1.9}Ga_{0.1}$ at 250 K and at 350 K, and $Gd_5Si_2Ge_{1.9}Cu_{0.1}$ at 200 K and at 350 K. Symbols: observed patterns. Black lines: calculated for the O(I) structure. Green ticks: positions of the Bragg reflections for three phases: main O(I) phase, $Gd(Si, Ge)_1$ and $Gd_5(Si, Ge)_3$. Green line: calculated for the M phase, according to structural data given in [7]. Arrows indicate some characteristic reflections for the O(I) and M structures.

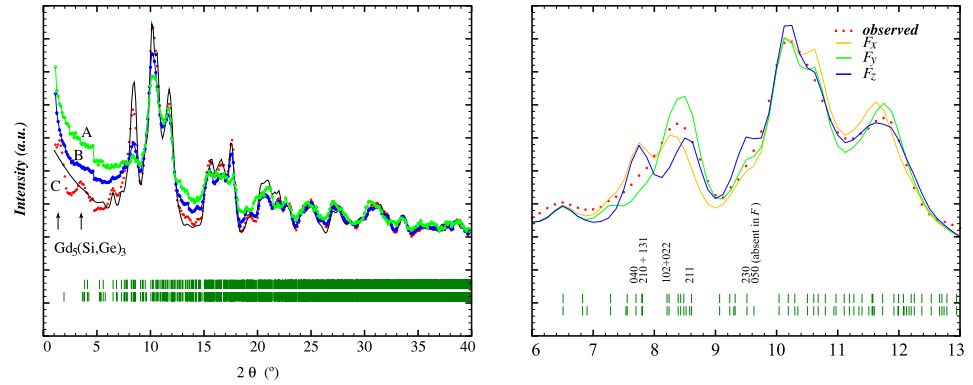

Figure 3. Left, symbols: observed neutron diffraction patterns of $Gd_5Si_2Ge_2$ at 310 K (A), 240 K (B) and 20 K (C). Ticks: positions of the Bragg peaks for the nuclear and magnetic scattering. Lines: calculated with structural parameters taken from XRD, for the ferromagnetic mode F_y (group $Pn'ma'$), with moments of 7 μ_B (black). Arrows indicate the bumps ascribed to the possible modulated structure of the 5:3 phase. Right: magnified portion of the 20 K pattern, indicating some key reflections. Lines: calculated for the three ferromagnetic modes.

The sample was distributed over a hollow cylinder of 9 mm diameter and 0.5 mm thickness, suitable for an average absorption length of $L = 0.53$ mm corresponding to a solid $Gd_5Si_2Ge_2$ sample. The resolution, ca 0.2°, does not allow us to observe the individual reflections. Therefore the magnetic mode will be deduced by trial and error, comparing the observed pattern with the calculated one for every possible magnetic mode. The patterns (figure 3) were collected for all samples in the paramagnetic phase (above 300 K), a few kelvin below the transition (240 K) and at 20 K. The scattering length of natural Gd for $\lambda = 0.4964$ Å was interpolated between the nearest values in table 1 of [11], giving $b = (1.067 - i0.042) \times 10^{-12}$ cm. For Si, Ge, Ga and Cu, the usual values were taken, $(0.4149, 0.8185, 0.7288, 0.7718) \times 10^{-12}$ cm, as well as for the magnetic form factor of Gd.

The paramagnetic phase patterns are consistent with the structure derived from XRD, that is, M-type structure for $Gd_5Si_2Ge_2$ and O(I)-type for the doped alloys. In the non-doped sample the monoclinic distortion is not so evident as in the case of XRD because of the poorer resolution in the ND experiment, but in any case the Rietveld refinement gave acceptable reliability indices only for the M-type structure ($R_p = 0.014$, $R_{wp} = 0.018$, $\chi^2 = 1.19$, $R_{Bragg} = 0.015$, over raw data, not corrected for background). The 20 K pattern clearly shows an increase of the already present nuclear reflections. The most evident cases are the (121) at $2\theta = 6.51°$ (a rare case of a well separated reflection) and a group of eight reflections between $2\theta = 8.20°$ and 8.60°. The difference in the background is also evident and consistent with the incoherent paramagnetic scattering at 310 K. Two small bumps near 1.48° and 3.55° are supposed to correspond to the low temperature magnetic diffraction of the 5:3 phase, below 110 K [21]. From magnetic measurements the magnetic structure of the hexagonal Gd_5Si_3 at low temperature was supposed to be helical [22]. Recent single crystal ND experiments [23] showed a modulated structure with wavevector $\boldsymbol{k} = (0, 0, 0.40)$, therefore we can expect a peak at $2\theta = 1.8°$, but actually the 5:3 phase is composed of both Ge and Si and the propagation vector is not necessarily the same as in Gd_5Ge_3 (if the magnetic structures were the same). As additional tips to ascribe these bumps to the 5:3 phase we can notice that: (a) the bumps do not exist at 240 K, when the main phase is magnetically ordered (but not the 5:3 phase), and the heat capacity [16] does not reveal any other transition between 20 and 240 K. (b) The position of the bump at 1.48° does not correspond to any possible Bragg

Table 1. Magnetic irreducible representations for the 4c and 8d positions of the space group $Pnma$ with $\boldsymbol{k} = 0$ [25, 26].

Irrep	x	y	z	x	y	z	Group
Γ_1		C_y		C_{Bx}	G_{By}	A_{Bz}	$Pnma$
Γ_2	C_x		F_z	G_{Bx}	C_{By}	F_{Bz}	$Pn'm'a$
Γ_3	F_x		C_z	F_{Bx}	A_{By}	G_{Bz}	$Pnm'a'$
Γ_4		F_y		A_{Bx}	F_{By}	C_{Bz}	$Pn'ma'$
Γ_5	A_x		G_z	R_x	Q_y	L_z	$Pn'm'a'$
Γ_6		A_y		Q_x	R_y	P_z	$Pnma'$
Γ_7		G_y		P_x	L_y	Q_z	$Pn'ma$
Γ_8	G_x		A_z	L_x	P_y	R_z	$Pnm'a$

reflection with $\boldsymbol{k} = 0$, which could be ascribed to some kind of antiferromagnetic order. (c) The magnetization data give a magnetic moment per atom of 7.52 μ_B [24] for the very similar compound Gd_5Si_4, slightly above the theoretical spin-only value of 7 μ_B. That is hardly compatible with a helical or sinusoidal antiferromagnetic structure, which would give a zero net moment. Some modulation around a non-zero moment cannot be completely ruled out, but we keep the simplest hypothesis of a collinear structure with $\boldsymbol{k} = 0$ and constant moments. The magnetic irreducible representations (table 1) for the nuclear space group $Pnma$ and $\boldsymbol{k} = 0$ were given in [25], based on Bertaut's theory [26] and corresponding to the eight magnetic groups arising when the time inversion is combined with the space symmetry elements. In order to determine the magnetic group at 20 K we consider as a first approximation a fixed magnetic moment of 7 μ_B in each Gd site. There are three Gd atoms in the asymmetric unit at Wyckoff sites 4c, 8d and 8d of the crystallographic space group $Pnma$. Within a given magnetic group and for a collinear structure, we can choose the sign of one moment (for instance that of the 4c site) but two signs remain to be adjusted, which define the relative orientation (parallel or antiparallel) of two inequivalent moments at the 8d sites. That makes 32 possible magnetic modes, to be compared against the experimental pattern, one by one.

Let us consider first the non-doped compound at 20 K. The purely antiferromagnetic groups, corresponding to representations Γ_1 and Γ_5–Γ_8, give strong peaks at low angles, near $2\theta = 3.63°$ and 5.40°, or the peak (010) at $2\theta = 1.92°$, which would be well separated but are not actually observed. Moreover, differently to the cases of Tb_5Ge_4 [25, 8] or Gd_5Ge_4, antiferromagnetic order was not observed in magnetic measurements for $Gd_5Si_2Ge_2$. Therefore, let us assume as starting point one ferromagnetic collinear mode, Γ_2, as an example. The basis function of this representation is described by the symbol F_z, indicating a ferromagnetic configuration along the c-axis for the 4c moments. For the 8d sites, according to table 1, the possible moment configurations are the ones labelled as G_{Bx}, C_{By}, F_{Bz}, or several of them. We will shorten similarly the notation throughout the paper, i.e. Γ_3 (F_x) or Γ_4 (F_y). F_x gives a pattern similar to the observed one (figure 3, right), but produces a peak at $2\theta = 7.70°$ (due to the reflections (040) and (131) with the scattering vector $\boldsymbol{q}$ nearly parallel to the crystal b axis and perpendicular to the magnetic moments for this mode) much more intense than the values observed in this range. On the contrary, there is not enough intensity in the range $2\theta = 8.20°$–$8.40°$, produced by the reflections (102), (022), (201), (112) and (220), most of them with $\boldsymbol{q}$ nearly perpendicular to the b axis. F_z explains the intensity of the region $2\theta = 8.20°$–$8.40°$ but gives too much intensity in the range $2\theta \simeq 7.70°$ of the reflections (040) and (131) and not enough in the range $2\theta \simeq 8.40°$–$8.80°$ of the reflections (220) and (211). Finally the mode F_y (Γ_4 or $Pn'ma'$) gives a nice qualitative agreement with the experiment even with no refined structural parameters (figure 3, right).

The Rietveld refinement was made using the program FullProf [27] starting with the positional and cell parameters taken from XRD and the magnetic F_y mode with 7 μ_B for all the moments. Due to the bumps at low angle and considering negligible the information at high angles, only the range $5° < 2\theta < 40°$ (1226 nuclear and 1401 magnetic reflections) was considered for the refinement. The results are displayed in table 2 and figure 4, left.

It is worthwhile to remark that the refined values of the magnetic moments have a large standard deviation and lie below the expected values from magnetization measurements at the same temperature. The group $Pn'ma'$ also allows components of the moments perpendicular to b (labelled as A_{Bx} and C_{Bz} in table 1) which would correspond to a canted structure, as observed in other $R_5(Si, Ge)_4$ compounds, for instance for R = Tb [8] or Er [9]. In the present refinement, for R = Gd, the x or z components were included (refining the moments in spherical coordinates while maintaining the magnetic group) but the best fit corresponds to a non-canted structure, within the standard deviation. If there is some canting, it should be very small and well below the experimental sensitivity. Therefore, the magnetic structure corresponds simply to a collinear ferromagnet.

At 240 K the magnetic structure is the same, with smaller magnetic moments. The average microscopic magnetization can be determined from magnetic measurements by extrapolation of the isothermal magnetization curve to zero field. From figure 2 of [1], in $Gd_5Si_{1.72}Ge_{2.28}$ the magnetization value is about 130 A m^2 kg^{-1} at 242.2 K, which corresponds to an average moment of 4.6 μ_B/atom, in good agreement with the ND result of 4.0(3) μ_B (table 2).

The doped compounds have the same magnetic structure as $Gd_5Si_2Ge_2$ with slightly different parameters. Figure 4, right, shows the patterns of the three compounds studied at 20 K and table 2 contains the final Rietveld fitting parameters. In some cases, refining individual magnetic moments in different sites led to divergence; therefore they were constrained to be equal. As in the non-doped compound, components perpendicular to the b axis are below 1 μ_B and below the sensitivity of the experiment. In summary, the magnetic structure is quite similar to that of Er_5Si_4 at 3 K, that is, ferromagnetic with moments along b, but the crystal structure of the last compound is M-type [9]. The composition–temperature phase diagram of $Gd_5(Si, Ge)_4$ (figure 1) is similar to the one observed for $Tb_5(Si, Ge)_4$, but the magnetic structure is completely different, the moments being near the ac plane, non-collinear and undergoing a spin reorientation at low temperature for the Tb compound [8]. The monoclinic phase of $Pr_5Si_2Ge_2$ is also different since the moments lie along the a direction [28].

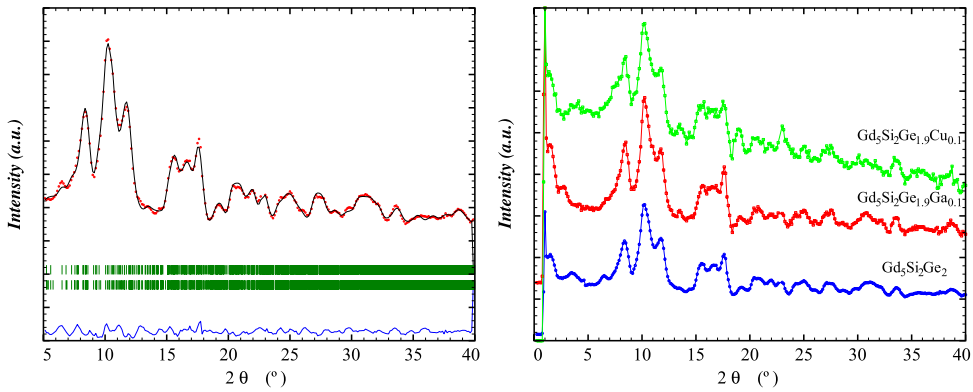

Figure 4. Left, symbols: observed ND pattern of $Gd_5Si_2Ge_2$ at 20 K. Lines: calculated after a Rietveld refinement with the parameters given in table 2 (black), and the difference (blue). Ticks: positions of the Bragg peaks for the nuclear and magnetic scattering. Right: observed ND patterns at 20 K for $Gd_5Si_2Ge_2$ and the doped compounds.

Table 2. Parameters of the Rietveld refinement of the ND patterns of $Gd_5Si_2Ge_{1.9}M_{0.1}$ (M = Ge means non-doped). Standard deviations in brackets, in units of the last digit. Tn = Si, Ge, Ga or Cu. Magnetic moments in Bohr magnetons. For M = Cu the coordinates were not refined. N_{par} is the number of refined parameters.

M, T		Ge, 20 K	Ge, 240 K	Ga, 20 K	Cu, 20 K
Gd1(4c)	x	0.355(3)	0.352(3)	0.380(3)	0.380
	y	1/4	1/4	1/4	1/4
	z	−0.018(2)	−0.017(2)	−0.002(4)	−0.002
Gd2(8d)	x	0.030 1(14)	0.031 3(15)	0.024(2)	0.024
	y	0.092 0(6)	0.092 1(7)	0.0963(10)	0.0963
	z	0.812 9(14)	0.811 4(17)	0.809(2)	0.809
Gd3(8d)	x	0.017 81(16)	0.018 08(19)	0.171(2)	0.171
	y	0.119 8(8)	0.121 3(9)	0.1217(12)	0.1217
	z	0.323 1(13)	0.321 1(15)	0.324(2)	0.324
T1(4c)	x	0.983(5)	0.984(5)	0.991(7)	0.991
	y	1/4	1/4	1/4	1/4
	z	0.099(5)	0.100(5)	0.067(7)	0.067
T2(4c)	x	0.265(5)	0.275(5)	0.269(9)	0.269
	y	1/4	1/4	1/4	1/4
	z	0.663(4)	0.663(4)	0.728(6)	0.728
T3(8d)	x	0.185(2)	0.185(2)	0.228(5)	0.228
	y	0.9487(12)	0.9488(12)	0.928(3)	0.928
	z	0.537(3)	0.538(3)	0.544(5)	0.544
μ(Gd1)		5.8(4)	3.2(4)	6.4(2)	7.3(4)
μ(Gd2)		6.4(3)	5.1(3)	6.4(2)	7.3(4)
μ(Gd3)		6.9(2)	3.4(3)	6.4(2)	7.3(4)
a (Å)		7.586(6)	7.603(7)	7.572(9)	7.64(2)
b (Å)		14.873(14)	14.895(15)	14.822(20)	14.77(5)
c (Å)		7.874(6)	7.894(8)	7.839(10)	7.87(2)
V (Å^3)		888.4(13)	894.0(15)	880.0(20)	887(4)
R_p/R_{wp} (%)		1.7/2.1	1.4/1.8	3.2/4.1	2.2/2.9
R_{Bragg}/R_{mag} (%)		2.2/3.2	2.1/3.2	4.9/5.4	11/8.7
χ^2		1.5	1.03	2.1	1.4
N_{par}		34	34	28	10

4. Conclusions

Previous heat capacity and direct magnetocaloric determinations [16] in $Gd_5Si_2Ge_{1.9}Ga_{0.1}$ have shown a substantially different behaviour compared to that of $Gd_5Si_2Ge_2$. In the doped compound there is no first-order transition but a usual second-order magnetic transition with similar T_C to the one of Gd_5Si_4. The heat capacity and the isothermal entropy increment are similar to the values for pure Gd, with a proper scaling due to the relative fraction of Gd atoms in the sample, and decreasing according to the MCE with respect to that of pure Gd. The high and low temperature XRD patterns support those results as they show the well known O(I) to M transition in $Gd_5Si_2Ge_2$ but not in the doped compounds, which remain in the O(I) phase across the magnetic transition. These conclusions agree with those given in [29] for $Gd_5Si_{2-y}Ge_{2-y}Ga_{2y}$ with $y \geqslant 0.05$ from DSC and magnetization data. The lower y value corresponds to the Ga amount of our compound, but in this case both Si and Ge are replaced by Ga.

The magnetic structure of $Gd_5Si_2Ge_2$ below T_C is the same as that of the doped compounds $Gd_5Si_2Ge_{1.9}M_{0.1}$ (M = Ga, Cu), collinear ferromagnetic F_yF_{By}, with the magnetic moments in the *b* direction of the *Pnma* space group. This is different and much simpler than for compounds with other rare earths (Er, Tb, Yb) substituting Gd. At 20 K the average magnetic moment, 6.5(3) μ_B/atom, lies slightly below the value derived from magnetization measurements (between 7.2 and 7.5 μ_B/atom, taken from the literature) which can be due to the low precision of the ND experiment or to the magnetic polarization of the conduction electrons.

For $Gd_5Si_2Ge_2$ at 240 K, just below the magnetostructural transition, the magnetic moment is considerably lower than the saturation value of 7 μ_B/atom. This is not surprising, although it has strong consequences for the MCE since the magnetic entropy in the ferromagnetic phase is already quite high at this temperature. Therefore the magnetic entropy jump per atom at the transition is well below the theoretical limit of $k_B \ln(2S+1)$. This imposes severe limitations for applications of these compounds in magnetic refrigeration. Mn or Fe compounds with a strong electronic contribution to the entropy jump at the transition have higher MCE than $Gd_5Si_2Ge_2$ in spite of their lower magnetic moments.

Acknowledgments

The authors acknowledge the Spanish MICINN and FEDER funding, projects MAT2007-61621 and CSD2007-00010, and ILL facilities, experiment no. 5-31-1944. We acknowledge V Provenzano and R D Shull for supplying the samples.

References

[1] Pecharsky V K and Gschneidner K A Jr 1997 *Phys. Rev. Lett.* **78** 4494–7
[2] Tishin A M and Spichkin Y I 2003 *The Magnetocaloric Effect and its Applications* (Bristol: IOP Publishing)
[3] Brück E, Tegus O, Cam Thanh D T, Trung Nguyen T and Buschow K H J 2008 *Int. J. Refrig.* **31** 763–70
[4] Mozharivskyj Y, Pecharsky A O, Pecharsky V and Miller G J 2005 *J. Am. Chem. Soc.* **127** 317–24
[5] Pecharsky V K and Gschneidner K A Jr 1997 *Appl. Phys. Lett.* **70** 3299–302
[6] Morellon L, Blasco J, Algarabel P A and Ibarra M R 2000 *Phys. Rev.* B **62** 1022–6
[7] Choe W, Pecharsky V K, Pecharsky A O, Gschneidner K A Jr, Young V G Jr and Miller G J 2000 *Phys. Rev. Lett.* **84** 4617–20
[8] Ritter C, Morellon L, Algarabel P A, Magen C and Ibarra M R 2002 *Phys. Rev.* B **65** 094405
[9] Ritter C, Magen C, Morellon L, Algarabel P A, Ibarra M R, Pecharsky V K, Tsokol A O and Gschneidner K A Jr 2006 *J. Phys.: Condens. Matter* **18** 3937–50
[10] *CRC Hanbook of Chemistry and Physics* 1997 77th edn (Boca Raton, FL: CRC Press)
[11] Abell J S, Boucherle J X, Osborn R, Rainford B D and Sweizer J 1983 *J. Magn. Magn. Mater.* **31–34** 247–8
[12] Barandiaran J M, Gignoux D, Schmitt D, Gomez-Sal J C, Rodriguez Fernandez J, Chieux P and Schweizer J 1988 *J. Magn. Magn. Mater.* **73** 233–9
[13] Blanco J A, Espeso J I, García Soldevilla J, Gómez Sal J C, Ibarra M R, Marquina C and Fischer H E 1999 *Phys. Rev.* B **59** 512–8
[14] Provenzano V, Shapiro A J and Shull R D 2004 *Nature* **429** 853–7
[15] Shull R D, Provenzano V, Shapiro A J, Fu A, Lufaso M W, Karapetrova J, Kleteschka G and Mikula V 2006 *J. Appl. Phys.* **99** 08K908
[16] Palacios E, Wang G F, Burriel R, Provenzano V and Shull R D 2010 *J. Phys.: Conf. Ser.* **200** 092011
[17] Fischer H E, Cuello G J, Palleau P, Feltin D, Barnes A C, Badyal Y S and Simonson J M 2002 *Appl. Phys.* A **74** S160–2
[18] Pecharsky V K and Gschneidner K A Jr 1997 *J. Alloys Compounds* **260** 98–106
[19] Choe W, Pecharsky A O, Woerle M and Miller G J 2003 *Inorg. Chem.* **42** 8223–9
[20] Misra S and Miller G J 2006 *J. Solid State Chem.* **179** 2290–7
[21] Podmiljsak B, Skulj I, Markoli B, Zuzek Rozman K, McGuiness P J and Kobe S 2009 *J. Magn. Magn. Mater.* **321** 300–4
[22] Ganapathy E V, Kugimiya K, Steinfink H and Tchernev D I 1976 *J. Less Common Metals* **44** 245–58
[23] Rotter M 2010 *V Meeting of the SETN* Gijón (Spain), private communication
[24] Spichkin Y I, Pecharsky V K and Gschneidner K A Jr 2001 *J. Appl. Phys.* **89** 1738–45
[25] Schobinger-Papamantellos P 1978 *J. Phys. Chem. Solids* **39** 197–205
[26] Bertaut E F 1963 *Spin Configuratios of Ionic Structures: Theory and Practice* (*Magnetism*) vol III, ed G T Rado and H Suhl (New York: Academic) p 149
[27] Rodríguez-Carvajal J 1993 *Physica* B **192** 55
Rodríguez-Carvajal and Roisnel T 1998 New Windows 95/NT applications for diffraction *Commission for Powder Diffraction Newsletter* 20 International Union for Crystallography p 35 http://www.iucr.org/_data/asset/pdf_file/0017/21635/cpd20.pdf
[28] Wang Y C, Yang H F, Huang Q, Duan L B, Lynn J W and Rao G H 2007 *Phys. Rev.* B **76** 064425
[29] Aksoy S, Yucel A, Elerman Y, Krenke T, Acet M, Moya X and Mañosa L 2008 *J. Alloys Compounds* **460** 94–8